PROCEEDINGS OF SCIENCE

Impact of muon detection thresholds on the separability of primary cosmic rays

Sarah Müller, Ralph Engel, Tanguy Pierog, Markus Roth*
Institut für Kernphysik, Karlsruhe Institute of Technology (KIT), Karlsruhe, Germany
E-mail: sarah.mueller2@kit.edu

Knowledge of the mass composition of cosmic rays in the transition region of galactic to extragalactic cosmic rays allows to discriminate different astrophysical models on their origin, acceleration, and propagation. An important observable to separate different mass groups of cosmic rays is the number of muons in extensive air showers. We performed a CORSIKA simulation study to analyze the impact of the detection threshold of muons on the separation quality of different primary cosmic rays in the energy region of the ankle. Using only the number of muons as the composition-sensitive observable, we find a clear dependence of the separation power on the detection threshold for ideal measurements. Although the number of detected muons increases when lowering the threshold, the discrimination power is reduced. If statistical fluctuations for muon detectors of limited size are taken into account, the threshold dependence remains qualitatively the same for small distances to the shower core but is reduced for large core distances. We interpret the impact of the detection threshold of muons on the composition sensitivity by the change of the correlation of the number of muons N_μ with the shower maximum $X_{\max}$ as function of the muon energy as a result of the underlying hadronic interactions and the shower geometry. We further investigate the role of muons produced by photon-air interactions and conclude that, in addition to the effect of the $N_\mu - X_{\max}$ correlation, the separability of primaries is reduced as a consequence of the presence of more muons from photonuclear reactions in proton than in iron showers.

35th International Cosmic Ray Conference — ICRC2017
10–20 July, 2017
Bexco, Busan, Korea

*Speaker.

© Copyright owned by the author(s) under the terms of the Creative Commons Attribution-NonCommercial-NoDerivatives 4.0 International License (CC BY-NC-ND 4.0).

PoS(ICRC2017)311

1. Introduction

To discriminate between different physics scenarios of the production and propagation of ultra-high energy cosmic rays, a precise measurement of their mass composition in the transition region of galactic to extragalactic cosmic rays up to ultra-high energies is necessary. An important mass related observable is the number of muons in extensive air showers [1]. The detection thresholds of muon detectors with limited size in air shower experiments that have obtained important composition results cover a range from 230 MeV for KASCADE [2] up to 10 GeV for the EAS-MSU main muon detector of [3]. Currently, also the Pierre Auger and the Telescope Array Collaborations are planning to extend their experiments by muon detectors of different types [4, 5].

In this work, we analyze the impact of the detection threshold of muons on the separability of extensive air showers for composition analyses based on pure CORSIKA simulations. Previous results have been shown in [6]. We make use of the fact that the number of muons in an extensive air shower depends on the mass of the primary cosmic ray particle such that heavier particles induce a significantly larger muon content [7]. Although larger detection thresholds of muons imply a reduced statistics, it is a priori not clear if low-energy muons help to discriminate better between air showers from different primary particles. To explain the observed dependence of the separability of primaries on the detection threshold of muons, we analyze the correlation of N_μ with $X_{\max}$ for different detection thresholds and distances to the shower core.

2. Methods

We used the CORSIKA software package [8] to perform full simulations of extensive air showers (no thinning applied) with primary energy 3.16×10^{18} eV, EPOS-LHC [9] as high interaction model, and zenith angle $\theta = 38^\circ$. 115 simulations were done for proton and iron primaries each. To analyze the dependence of the composition sensitivity on the detection threshold of muons for muon detectors of different sizes, we first determine the "true" muon densities in rings in the shower plane by $\rho_\mu = \frac{N_{\text{ring}}}{\pi\left((r+\delta r)^2 - r^2\right)}$ for each CORSIKA simulation and each detection threshold. Here, N_{ring} denotes the total number of muons with projected coordinates inside the ring with inner and outer radii r and $r+\delta r$, respectively. We assume no significant azimuthal asymmetries being present. Then, we account for fluctuations in the number of muons falling inside the detection area A by sampling from a Poissonian distribution $P_\lambda(k) = \frac{\lambda^k}{k!} e^{-\lambda}$ with $\lambda = \rho_\mu A$ equals the expected number of muons. We model the uncertainties in $X_{\max}$ by sampling from Gaussian distributions around the CORSIKA $X_{\max}$ values with standard deviation $\sigma(X_{\max}) = 20\,\text{g/cm}^2$, which corresponds approximately to the resolution of the fluorescence detectors of the Pierre Auger Observatory [10] at the energy of the ankle. We quantify the impact of the detection threshold of muons on the separability between extensive air showers of proton and iron primary cosmic rays, based on the number of muons only, by the figure of merit $f_N = \frac{\overline{N}_{\text{Fe}} - \overline{N}_{\text{p}}}{\sqrt{\sigma^2_{N,\text{p}} + \sigma^2_{N,\text{Fe}}}}$. Means $\overline{N}_{\text{p}}$ ($\overline{N}_{\text{Fe}}$) and uncertainties $\sigma_{N,\text{p}}$ ($\sigma_{N,\text{Fe}}$), originating from both the finite detector size and the stochastic nature of the first interaction and subsequent shower development, are determined for each detection threshold of muons, radial distance to the shower core, and detection area. Additionally, we analyze the dependence of the composition sensitivity on the detection threshold of muons for a bivariate

PoS(ICRC2017)311

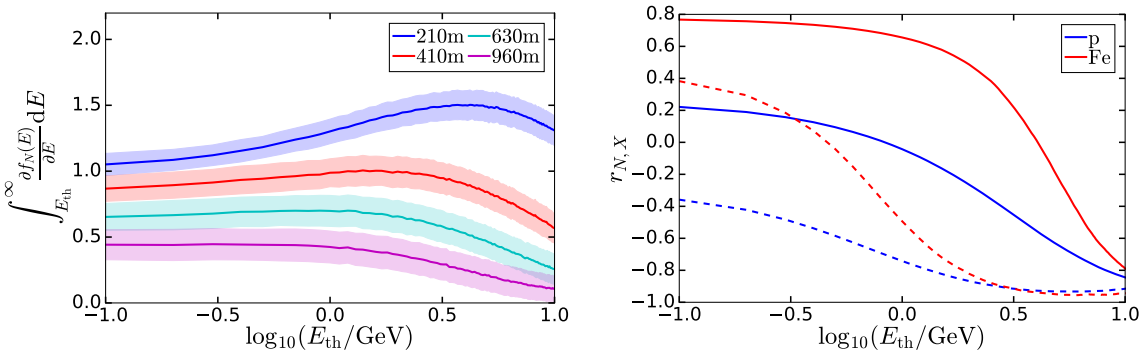

Figure 1: Left: Figure of merit f_N as a function of the detection threshold E_{th} for different radial distances and a detection area of $10\,\mathrm{m}^2$. Shaded bands denote the 1σ uncertainties. Right: Pearson product-moment correlation coefficient $r_{N,X} = \frac{\mathrm{cov}(N_\mu, X_{\mathrm{max}})}{\sigma_{N_\mu}\sigma_{X_{\mathrm{max}}}}$ based on "true" N_μ and X_{max} values for proton and iron showers as a function of E_{th} for $r = 210\,\mathrm{m}$ (solid lines) and $r = 960\,\mathrm{m}$ (dashed).

composition analysis using both the N_μ and X_{max} information. We employ the square-root of the maximal Fisher discriminant ratio $f_{N-X} \equiv \sqrt{\max_{\vec{\omega}\neq 0} f} = \sqrt{\left(\vec{\mu}_{\mathrm{p}} - \vec{\mu}_{\mathrm{Fe}}\right)^{\top} \left(\hat{\Sigma}_{\mathrm{p}} + \hat{\Sigma}_{\mathrm{Fe}}\right)^{-1} \left(\vec{\mu}_{\mathrm{p}} - \vec{\mu}_{\mathrm{Fe}}\right)^{\top}}$ to quantify the separation between the proton and iron primary classes separated by the linear discriminant $\vec{\omega}^{\mathrm{max}} = \left(\hat{\Sigma}_{\mathrm{p}} + \hat{\Sigma}_{\mathrm{Fe}}\right)^{-1} \left(\vec{\mu}_{\mathrm{p}} - \vec{\mu}_{\mathrm{Fe}}\right)$ where $\vec{\mu}_{\mathrm{p}} = \left(\overline{N}_{\mathrm{p}}, X^{\mathrm{p}}_{\mathrm{max}}\right)^T$ ($\vec{\mu}_{\mathrm{Fe}}$) and $\hat{\Sigma}_{\mathrm{p}}$, ($\hat{\Sigma}_{\mathrm{Fe}}$) are the vectors of the means and the covariance matrices of the two classes.

3. Results

The dependence of the composition sensitivity on the detection threshold of muons is shown in Fig. 1 left for a detection area of $A = 10\,\mathrm{m}^2$ and different radial distances to the shower core. It is surprising that the optimum separation power for f_N, based on the number of muons only, is not found for the lowest energy threshold for which the number of detected muons is largest and correspondingly the detection fluctuations are smallest. Instead, the best separation of primaries is obtained for thresholds of about 4.2 GeV for a small core distance of $r = 210\,\mathrm{m}$ and a detection area of $10\,\mathrm{m}^2$.

Statistical uncertainties in the detected number of muons increase with decreasing muon densities. This leads to a reduction of the composition sensitivity for larger distances to the shower core and, for smaller detection areas (see Fig. 2), additionally to a shift of the optimal detection threshold towards smaller values. The fact that maximum separability for f_N is achieved for thresholds of a few GeV at small core distances, instead of lowest considered thresholds, is hence not a consequence of the limited statistics of detected muons but on the contrary a result of the underlying physics which will be explored in more detail in the following. The Fisher discriminant ratio f_{N-X}, shown in Fig. 2 right, has a similar dependence on the detection threshold of muons as f_N for true $N_\mu - X_{\mathrm{max}}$ values, although the composition sensitivity is less reduced for lowest thresholds.

3.1 Dependence of composition sensitivity on $\mathbf{N_\mu - X_{max}}$ correlation

In order to explain the dependence of f_N and f_{N-X} on the detection threshold of muons, we first consider the correlation of the "true" N_μ and X_{max} values and later come back to the impact

PoS(ICRC2017)311

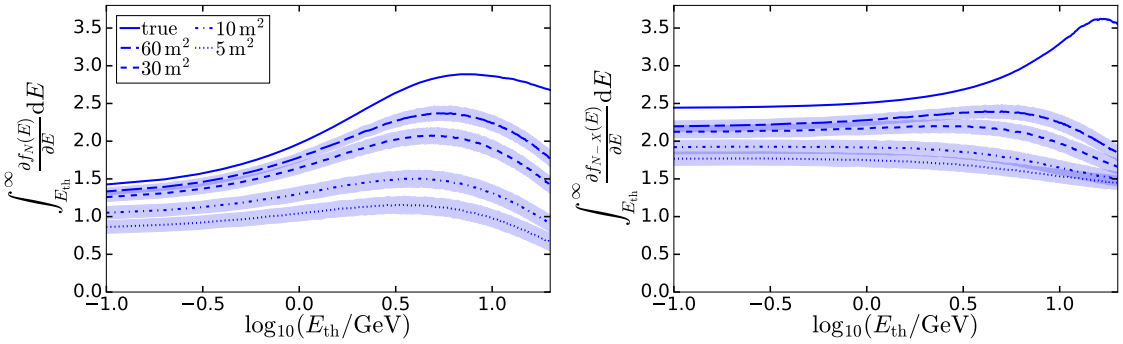

(a) $r = 210\,\mathrm{m}$

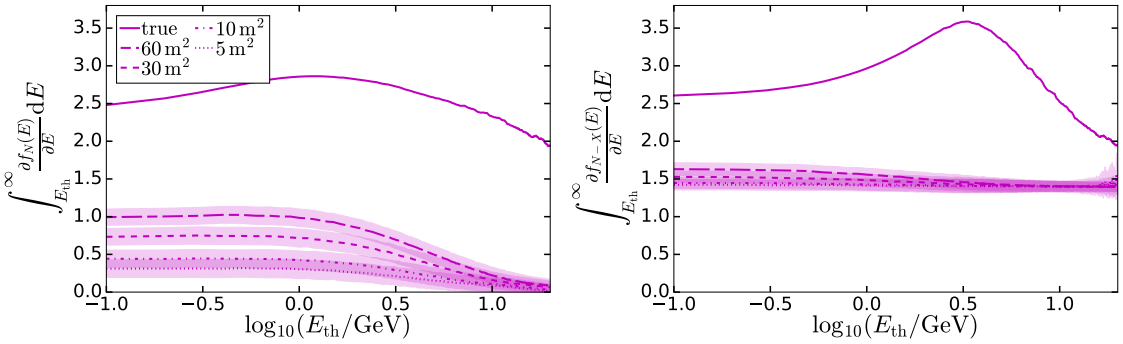

(b) $r = 960\,\mathrm{m}$

Figure 2: Figure of merit f_N (left) and Fisher discriminant ratio f_{N-X} (right) for core distances $r = 210\,\mathrm{m}$ (top) and 960 m (bottom) as a function of the detection threshold of muons E_{th} for different muon detector sizes of $A = 5, 10, 30\,\mathrm{m}^2$ and $60\,\mathrm{m}^2$ compared to results for "true" N_μ and X_{max} values.

of statistical fluctuations. For a small detection threshold of $E_{\mathrm{th}} = 0.1\,\mathrm{GeV}$ (Fig. 3a), the number of muons and the shower maximum are positively correlated for both iron and proton showers; for increasing thresholds, the ellipses rotate and the correlation changes from positive to negative (Fig. 3b). The Pearson correlation coefficients $r_{N,X}$ of $N_\mu - X_{\mathrm{max}}$ are shown as a function of the detection threshold of muons in Fig. 1 right for core distances $r = 210\,\mathrm{m}$ and $r = 960\,\mathrm{m}$. Since proton showers generally have larger X_{max} values than iron showers, the positive $N_\mu - X_{\mathrm{max}}$ correlation for proton showers for $E_{\mathrm{th}} = 0.1\,\mathrm{GeV}$ and $r = 210\,\mathrm{m}$ causes an almost complete overlap of the muon number distribution for iron with the proton distribution leading to reduced f_N values for small detection thresholds. The composition sensitivity increases with the turning of the $N_\mu - X_{\mathrm{max}}$ ellipses for increasing thresholds due to the reduced overlap of the proton and iron muon number distributions. For high thresholds (at the order of 16 GeV for $r = 210\,\mathrm{m}$ and without measurement fluctuations considered), the increasing negative correlation for both primaries causes again an overlap of muon numbers for shallow proton showers and deep iron showers and hence a reduction of the composition sensitivity based on muon numbers only.

The correlation coefficients $r_{N,X}$ for a large core distance of $r = 960\,\mathrm{m}$ are shifted towards smaller values compared to $r = 210\,\mathrm{m}$. At smallest thresholds of 0.1 GeV, proton showers already

PoS(ICRC2017)311

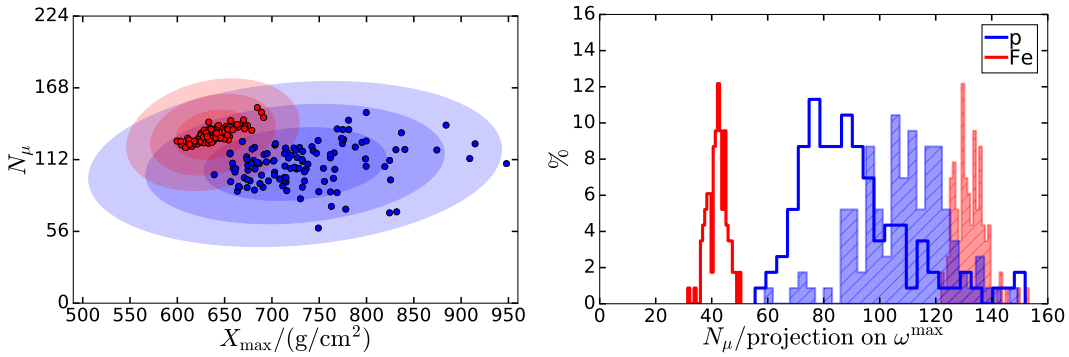

(a) $E_{\mathrm{th}} = 0.1\,\mathrm{GeV}$

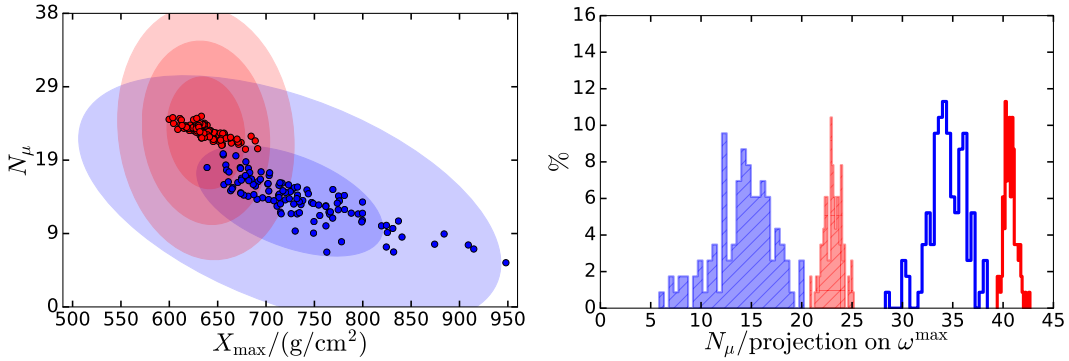

(b) $E_{\mathrm{th}} = 10\,\mathrm{GeV}$

Figure 3: Left: $N_\mu - X_{\max}$ distributions for detection thresholds of muons of $E_{\mathrm{th}} = 0.1\,\mathrm{GeV}$ and $10\,\mathrm{GeV}$ at $r = 210\,\mathrm{m}$. Scatter points for iron (red) and proton showers (blue) correspond to the "true" N_μ and $X_{\max}$ values. Additionally, the $1, 2$, and 3σ uncertainty ellipses due to measurement uncertainties are displayed for a muon detection area of $A = 10\,\mathrm{m}^2$. Right: projections of the true $N_\mu - X_{\max}$ distributions (points on the left hand side) on the N_μ-axis (shaded histograms) and the optimal Fisher discriminants (solid histogram lines). Note that the flip in ordering of the projected proton and iron distributions is due to the changing orientation of the Fisher discriminant.

have a negative $N_\mu - X_{\max}$ correlation ($r_{N,X} = -0.36$), while iron showers are positively correlated ($r_{N-X} = 0.38$). Hence, the true muon number distributions without any statistical fluctuations accounted for do not overlap. The increase of separation power between primaries as a function of the detection threshold of muons, based on the number of muons only, is consequently much less pronounced then for a small core distance of $r = 210\,\mathrm{m}$.

Bivariate Fisher discriminant analyses, based on both N_μ and $X_{\max}$, are virtually not affected by the overlapping muon number distributions for small detection thresholds of muons, since the optimal Fisher discriminant axis is chosen such that the separation between the projected distributions is maximized. Nevertheless, thresholds of 16.2 GeV ($r = 210\,\mathrm{m}$) and 3.3 GeV (960 m) are favored based on true N_μ and $X_{\max}$ values (see Fig. 2 right). If statistical fluctuations are taken into account, there is only a slight preference for thresholds of a few GeV near to the shower core and for detection areas $\geq 30\,\mathrm{m}^2$; otherwise lowest thresholds yield equivalently good results.

For composition analyses based on the number of muons only, lowest detection thresholds

PoS(ICRC2017)311

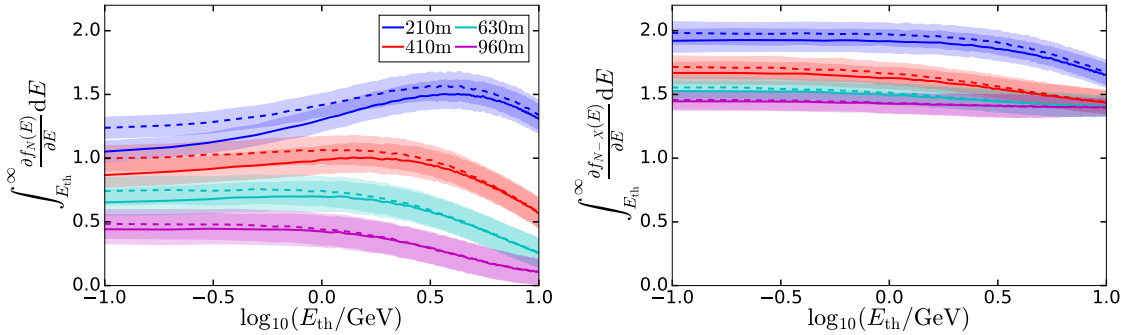

Figure 4: Figure of merit f_N (left) and Fisher discriminant ratio f_{N-X} (right) as a function of E_{th} if all muons are taken into account (solid lines) and if only muons without any preceding photonuclear interaction are considered (dashed) for $A = 10\,\text{m}^2$. Uncertainties are displayed by shaded bands.

are favored in the case of large fluctuations of N_μ, i.e. far from the shower core and for small detection areas. However, for smaller core distances, the dependence on the detection threshold of muons is clearly visible for all considered detection areas $\geq 5\,\text{m}^2$. At lowest thresholds, statistical uncertainties play a minor role and the separation power is almost completely determined by the overlapping muon number distributions as a result of the positive $N_\mu - X_{\text{max}}$ correlation for proton showers. Thresholds of $3.6-5.1\,\text{GeV}$ $(5-60\,\text{m}^2)$ yield optimal results for the considered primary energy.

3.2 Geometrical interpretation of $\mathbf{N_\mu - X_{max}}$ correlation

The dependence of the $N_\mu - X_{\text{max}}$ correlation on the detection threshold of muons and distance to the shower core can be qualitatively explained by the distribution in transverse momentum of muons that are produced in hadronic interactions during the shower development. The differential muon number distribution in momentum space can be estimated from hadronic interaction models by $\frac{\mathrm{d}^2 N_\mu}{\mathrm{d}^2\vec{p}_\perp} = \frac{\mathrm{d}^2 N_\mu}{\mathrm{d}\varphi p_\perp \mathrm{d}p_\perp} = \frac{N_\mu^{\text{tot}}}{2\pi p_{\perp_0}} e^{-\frac{p_\perp}{p_{\perp_0}}}$, where $\vec{p}_\perp$ designates the transverse momentum w.r.t. the shower axis ($p_\perp = |\vec{p}_\perp|$), $p_{\perp_0} = \langle p_\perp \rangle \approx 350-400\,\text{MeV}$ the average transverse momentum [1, 11] and N_μ^{tot} the total number of muons.

The atmospheric slant depth $X_{\mu_{\text{max}}}^{\text{prod}}$, where the production of muons is maximal, is related to the slant depth of the electromagnetic shower maximum by $X_{\mu_{\text{max}}}^{\text{prod}} \approx X_{\text{max}}^{\text{em}} + \Delta$ with $\Delta \approx 200\,\text{g}\,\text{cm}^{-2}$ [12]. For a muon produced at slant depth $X_{\mu_{\text{max}}}^{\text{prod}}$ and hitting the ground at core distance r without any intermediate interactions, the transverse muon momentum $p_\perp$ can be related to the total muon momentum p_μ, the distance to the shower core r in the shower plane and the geometrical distance R along the shower axis from the point of production to the intersection of the shower axis and the ground plane by $p_\perp = p_\mu \frac{r}{R}$. Here, the geometrical relations $\tan\theta_\mu = \frac{r}{R} \approx \theta_\mu$ and $\sin\theta_\mu = \frac{p_\perp}{p_\mu} \approx \theta_\mu$ for the angle θ_μ between the muon momentum and the shower axis and $r \ll R$ and $p_\perp \ll p_\mu$ have been used. The muon number density in the shower plane can hence be expressed by

$$\frac{\mathrm{d}^2 N_\mu}{\mathrm{d}^2\vec{r}} = \frac{\mathrm{d}^2 N_\mu}{\mathrm{d}^2\vec{p}_\perp}\frac{\mathrm{d}^2\vec{p}_\perp}{\mathrm{d}^2\vec{r}} = N_\mu^{\text{tot}} \frac{p_\mu^2}{2\pi p_{\perp_0} R^2} e^{-\frac{p_\mu}{p_{\perp_0} R} r}. \tag{3.1}$$

PoS(ICRC2017)311

From Eq. 3.1 follows that LDFs steepen for larger depths of the electromagnetic shower maximum. Consequently, there is a crossing of LDFs for showers of different $X_{\max}$ values at some radial distance to the shower core which depends on the detection threshold of muons and the $X_{\max}$ range. At the intersection point r_{cross}, the number of muons is uncorrelated to the position of the shower maximum. For core distances $r > r_{\text{cross}}$, the $N_\mu - X_{\max}$ correlation is negative, while it is positive for $r < r_{\text{cross}}$. For a fixed radial distance r, it can be derived from Eq. 3.1 that the $N_\mu - X_{\max}$ correlation decreases with increasing muon energy as shown in Fig. 1.

3.3 Photonuclear interactions

In addition to the geometrical explanation of the dependence of the composition separability on the detection threshold of muons, we analyze the impact of muons produced by electromagnetic $\mu^+\mu^-$ pair creation processes $\gamma + \text{air} \rightarrow \mu^+\mu^-$ or hadronic photon-air interactions (photoproduction) of the type $\gamma + \text{air} \rightarrow \text{hadron/meson} + X$ with subsequent decay of the hadron or meson into a muon. Since extensive air showers initiated by a nucleus with atomic number A can be considered as a superposition of air showers induced by A nucleons with reduced energy E/A, less interaction generations and consequently less energy loss in electromagnetic interactions is predicted. While more muons from the hadronic part of the shower are expected for primaries with large A compared to proton induced showers [7], less electromagnetic interactions could lead to a simultaneous reduction in the number of muons produced by photonuclear interactions. We track these muons by increasing the "hadronic generation counter" (defined for the EHISTORY option [13] in CORSIKA) by a unique value every time a photonuclear reaction takes place in the preceding interaction chain.

We show the impact of muons from photonuclear reactions on both the figure of merit f_N and on the Fisher discriminant ratio f_{N-X} in Fig. 4. The f_N and f_{N-X} values which would be obtained if muons from photonuclear reactions could be excluded are shown by dashed lines for comparison. The largest difference can be seen for the lowest detection threshold of $E_{\text{th}} = 0.1\,\text{GeV}$ at distance $r = 210\,\text{m}$ from the shower core. Here, the figure of merit decreases from $f_{\text{w/o phn}} = 1.24 \pm 0.08$ to $f = 1.04 \pm 0.08$ if muons resulting from preceding photonuclear interactions are taken into account. For higher thresholds, the impact of muons from photonuclear reactions becomes less important. Likewise, the figures of merit f and $f_{\text{w/o phn}}$ approach each other for increasing distances to the shower core. The Fisher discriminant ratio f_{N-X} improves less by omitting muons from photonuclear reactions than the figure of merit f_N. It is shifted up by a constant offset for small detection thresholds of muons; for high thresholds, where Poissonian uncertainties lead to a reduction of the separability, the influence of muons from photonuclear reactions vanishes.

4. Summary

We have presented a CORSIKA simulation study to evaluate the impact of the detection threshold of muons on the separability of extensive air showers initiated by protons and iron nuclei. Surprisingly, optimum separation power, based on the number of muons only, is generally not found for the lowest energy threshold for which detection fluctuations are smallest but for thresholds of 4.2 GeV for distances close to the shower core and a detection area of $10\,\text{m}^2$. We identify the

PoS(ICRC2017)311

positive $N_\mu - X_{\max}$ correlation for proton showers at small core distances and low detection thresholds of muons as the reason for a large overlap of the iron and proton muon number distributions, causing a reduced separation power. Optimum separation power, without accounting for detection uncertainties, is found for higher thresholds where N_μ and $X_{\max}$ are negatively correlated without any overlap. If detection uncertainties in N_μ are taken into account, the composition sensitivity is reduced as the detection area decreases. In the case of small detection areas and large core distances, where composition sensitivity is small, lowest possible detection thresholds are therefore favored. However, for closer distances to the shower core, detection thresholds of $3.6 - 5.1\,\mathrm{GeV}$ ($5 - 60\,\mathrm{m}^2$) still yield best composition sensitivity as a consequence of the change in $N_\mu - X_{\max}$ correlation. We have demonstrated that the dependence of the $N_\mu - X_{\max}$ correlation on the core distance and detection threshold of muons can be qualitatively explained within a simple model for hadronic interactions and the shower geometry. Furthermore, we have analyzed the impact of muons produced by photon-air collisions on the separability of primaries. Besides the change in $N_\mu - X_{\max}$ correlation, these muons lead to a further reduction of the composition separability.

References

[1] R. Engel, D. Heck, and T. Pierog, *Extensive Air Showers and Hadronic Interactions at High Energy*, *Annual Review of Nuclear and Particle Science* **61** (2011), no. 1 467–489.

[2] T. Antoni et al., *The cosmic-ray experiment KASCADE*, *Nucl. Instrum. Meth. A* **513** (2003) 490–510.

[3] Y. A. Fomin, N. N. Kalmykov, I. S. Karpikov, G. V. Kulikov, M. Y. Kuznetsov, G. I. Rubtsov, V. P. Sulakov, and S. V. Troitsky, *Full Monte-Carlo description of the Moscow State University Extensive Air Shower experiment*, *JINST* **11** (2016), no. 08 T08005.

[4] R. Engel, The Pierre Auger Collaboration, *The Pierre Auger Observatory: Contributions to the 34th International Cosmic Ray Conference (ICRC 2015)*, *PoS* **ICRC2015** (2015) 136.

[5] T. Nonaka, The Telescope Array Collaboration, *Performance and Operational Status of Muon Detectors in the Telescope Array Experiment*, *PoS* **ICRC2015** (2015) 656.

[6] S. Müller and M. Roth, *A CORSIKA study on the influence of muon detector thresholds on the separability of primary cosmic rays at highest energies*, *PoS* **ICRC2015** (2015) 419.

[7] J. Matthews, *A Heitler model of extensive air showers*, *Astropart. Phys.* **22** (2005) 387–397.

[8] D. Heck, J. Knapp, J. N. Capdevielle, G. Schatz, T. Thouw, and Others, *CORSIKA: A Monte Carlo code to simulate extensive air showers*, *FZKA* **6019** (1998).

[9] T. Pierog and K. Werner, *EPOS Model and Ultra High Energy Cosmic Rays*, *Nucl. Phys. B - Proc. Suppl.* **196** (2009) 102–105.

[10] The Pierre Auger Collaboration, *Depth of maximum of air-shower profiles at the Pierre Auger Observatory. I. Measurements at energies above $10^{17.8}\,eV$*, *Physical Review D* **90** (2014).

[11] P. D. B. Collins and A. D. Martin, *Hadron reaction mechanisms*, *Reports on Progress in Physics* **45** (1982) 335.

[12] S. Andringa, L. Cazon, R. Conceição, and M. Pimenta, *The muonic longitudinal shower profiles at production*, *Astroparticle Physics* **35** (2012), no. 12 821–827.

[13] D. Heck and R. Engel, *The EHISTORY and MUPROD Options of the Air Shower Simulation Program CORSIKA*, *KIT-SWP* **5** (2009).

PoS(ICRC2017)311